INEEL/EXT-01-01643
Revision 0

Summary Report: Simulation of Groundwater Flow near the Subsurface Disposal Area at the Idaho National Engineering and Environmental Laboratory

April 2001

Idaho National Engineering and Environmental Laboratory
Bechtel BWXT Idaho, LLC

INEEL/EXT-01-01643
Revision 0

Summary Report: Simulation of Groundwater Flow near the Subsurface Disposal Area at the Idaho National Engineering and Environmental Laboratory

D. L. Whitmire
North Wind Environmental

April 2001

Idaho National Engineering and Environmental Laboratory
Environmental Restoration Program
Idaho Falls, Idaho 83415

Prepared under Subcontract No. K00-583018-032
for the
U.S. Department of Energy
Assistant Secretary or Office of Environmental Management
Under DOE Idaho Operations Office
Contract DE-AC07-99ID13727

Note: This document was produced for the Idaho National Engineering and Environmental Laboratory (INEEL) by an external subcontractor, and may not have been technically reviewed or edited to meet the INEEL publications standard. Also note that this document is Revision 0 under the assigned INEEL external report number but is Revision 1 under North Wind Environmental's documentation system.

North Wind Environmental

Revision 1
April 2001

Summary Report: Simulation of Groundwater Flow near the Subsurface Disposal Area at the Idaho National Engineering and Environmental Laboratory

D.L. Whitmire

ABSTRACT

A groundwater flow modeling study was undertaken in an effort to improve the accuracy of previous saturated-zone transport simulations. Deviation-corrected water level data and pump-test permeability information were used to discretize several TETRAD simulations. An optimal model run was selected for future use based on its quantitative fit to measured water levels, its inclusion of new data, its ability to incorporate mass flux information from the vadose zone, and its qualitative fit to water level trends in the vicinity of the Subsurface Disposal Area (SDA).

Prior to the development of the best-case simulation, permeability data were kriged and input to a TETRAD data deck in order to determine whether or not sufficient pump-tested permeability data exist to accurately simulate groundwater flow beneath the RWMC. Due to a short spatial correlation range and very few data points (i.e., pump-tested wells), the kriged permeability distribution did not produce an accurate simulation of observed hydraulic heads. Additional permeability data are necessary if a geostatistical approach toward permeability parameterization is attempted in future modeling efforts.

In order to assess the effects of infiltration of water from the spreading areas located west of the RWMC, infiltration rates were estimated and input to a TETRAD data deck (containing the best-case permeability distribution) in a high infiltration rate and low infiltration rate scenario. Both cases produced results that imply that groundwater flow directions are shifted southeastward upon addition of water to the spreading areas. Water levels observed during periods when water was added to the spreading areas imply the same trend. However, simulated water levels did not rise as dramatically as field measured water levels during the 1982 to 1985 time period.

CONTENTS

FIGURES

TABLES

ACRONYMS

ANL-W	Argonne National Laboratory-West
CFA	Central Facilities Area
INEEL	Idaho National Engineering and Environmental Laboratory
INTEC	Idaho Nuclear Technology and Engineering Center
MAE	Mean Absolute Error
ME	Mean Error
NRF	Naval Reactor Facility
RMS	Root Mean Square (Error)
RWMC	Radioactive Waste Management Complex
SDA	Subsurface Disposal Area
TAN	Test Area North
TRA	Test Reactor Area

1. INTRODUCTION

This report presents the development and calibration of a groundwater flow model that will be coupled with numerical simulations of water and contaminant flux through the vadose zone beneath the Subsurface Disposal Area (SDA). This modeling effort builds on previous simulation work performed for the SDA (Magnuson and Sondrup, 1998). Additional data have been collected since the previous modeling work; therefore, the simulations presented here are the most data-intensive representations of groundwater flow in the eastern Snake River Plain Aquifer (ESRPA) beneath the SDA developed to date.

1.1 Background

The SDA is part of the Radioactive Waste Management Complex (RWMC) located in the southwest portion of the Idaho National Engineering and Environmental Laboratory (INEEL) (Figure 1-1). Transuranic and mixed-wastes have been stored in subsurface

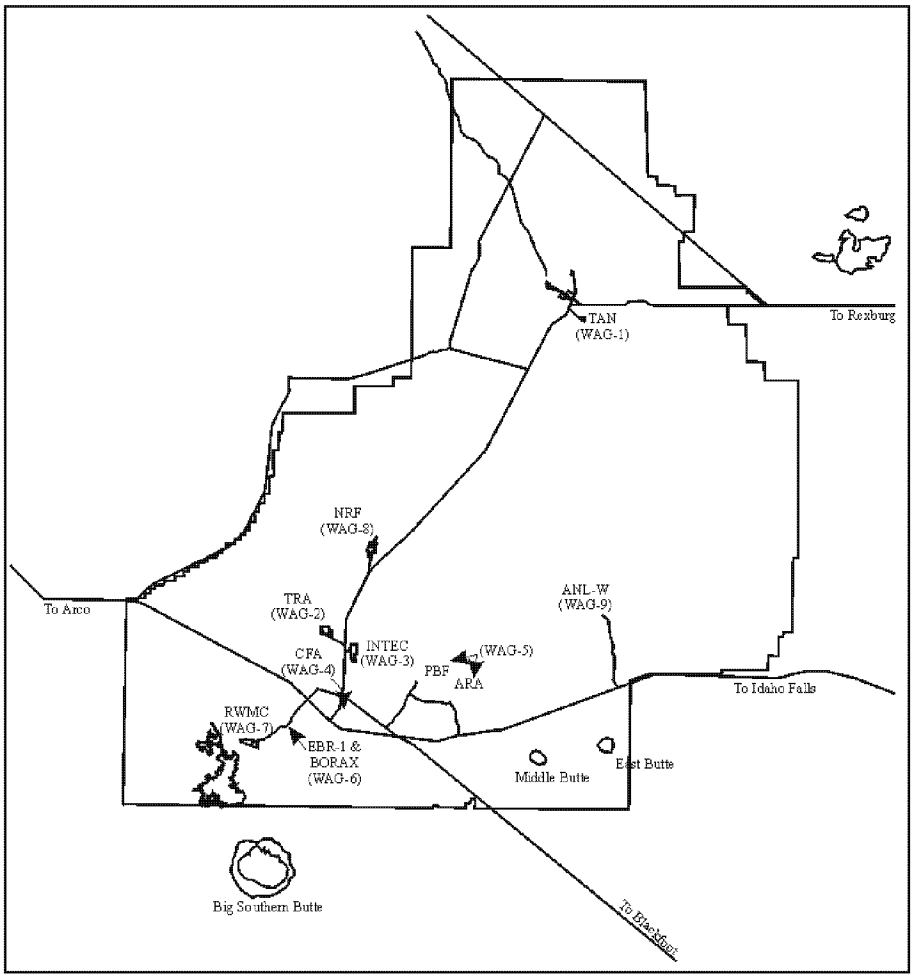

Figure 1-1. Map of the INEEL showing the location of the RWMC, INTEC, and CFA.

disposal pits and trenches at the SDA as recently as 1982. Low-level wastes continue to be buried in a portion of the SDA.

The SDA overlies a thick stratigraphic sequence composed primarily of fractured basalt flows interbedded with thinner sedimentary units (interbeds) that were deposited during periods of relative volcanic quiescence (Magnuson and Sondrup, 1998). The ESRPA underlies the SDA beginning at a depth of approximately 580 ft (176.8 m) below land surface. Numerous wells have penetrated both the vadose zone and the aquifer in the southern INEEL in an effort to characterize water and contaminant migration in the vicinity of several facilities including the RWMC, the Central Facilities Area (CFA), and the Idaho Nuclear Technology and Engineering Center (INTEC).

1.2 Purpose and Scope

The purpose of this study is to develop a calibrated groundwater flow model that can be used by BBWI staff during simulations of contaminant transport beneath the SDA. This modeling study is different from previous groundwater flow models (Magnuson and Sondrup, 1998) at the SDA in that it includes data that did not exist during previous investigations.

This report includes discussions of data gathering, conceptual model development, discretization, and calibration of the flow model to observed aquifer hydraulic heads. Further, this report describes the ability of the aquifer model to be coupled with mass flux output from a simulation of flow in the vadose zone. This report does not discuss the development or calibration of the vadose zone model; however, the calibration of the aquifer model is dependent upon the accuracy of the vadose zone model inasmuch as the mass flux of water in the vadose zone might affect water levels in the saturated zone.

1.3 Simulation Approach

This section provides an overview of the approach used to simulate groundwater flow beneath the SDA. The simulation code used during this study is described first. A summary of the procedures and goals used during the development and calibration of the model follows. Special emphasis is placed on the discussion of improvements to this model over past groundwater modeling efforts at the SDA.

1.3.1 Simulation Code

The TETRAD code (Vinsome and Shook, 1993) was chosen in order to maintain consistency with past modeling efforts at the SDA and in order to assure synergy when the aquifer model is coupled with the vadose zone model. The proficiency of TETRAD for modeling subsurface water and contaminant transport has been demonstrated in the past (Magnuson and Sondrup, 1998).

TETRAD uses a grid-centered, finite-difference approach and has multi-component, multi-phase simulation capabilities. Another important feature incorporated into the code is the capability for localized grid refinement. This feature allowed seamless matching of the modeled vadose zone domain with a portion of the aquifer domain.

1.3.2 Guidelines and Objectives

The following guidelines and objectives were used in order to measure the success of this study:

- The groundwater flow model must include water level and permeability data from wells that did not exist during previous simulation efforts.
- A portion of the aquifer model domain must match the vadose zone model domain at a scale of 1:1.
- Data should be evaluated to assure that only those that are truly representative of field conditions are used during model development.
- Based on currently available data, the model developed during this study should show an improvement over past simulations as measured with common quantitative calibration statistics (i.e. root mean square, mean absolute error, and mean error).
- It must be possible to incorporate mass flux information from the vadose zone model of the SDA subsurface into the aquifer model developed here.
- Where possible, the model developed during this study should maintain approximate consistency with past model geometries. As an example, the permeability distribution selected for this model should approximate the permeability distribution used during past modeling studies to the extent that is supported by data contained in the more complete dataset used during this study.
- Geostatisically analyzed permeability information should be input to the model domain during at least one model run in order to determine whether or not sufficient permeability data exist to generate a desirable simulation according to criteria discussed in sections 1.3.6.1 and 1.3.6.2 of this report.

1.3.3 Overview of Modeling Approach

The modeling study was conducted in several distinct stages: data gathering, data evaluation, model development, and model calibration. Water level data (corrected for deviation from vertical, where available) and aquifer hydraulic test information were gathered from resources available at the INEEL's Hydrologic Data Repository (HDR). Data that were found to be aberrant (based on deviation from their nearest neighbors) were investigated to determine whether or not any physical reasons exist that might explain their deviation from the expected pattern. Several data points were excluded from the dataset after potential data collection errors were discovered. The exclusion of these data is discussed in section 2 of this report.

After including mass flux of water from the base of the vadose zone (and into the aquifer) the groundwater flow model described in this report was calibrated versus observed, deviation-corrected hydraulic heads measured during 2000. An approximation of a "best" model run produced during the most recent SDA model calibration effort (Magnuson and Sondrup, 1998) was setup using the boundary conditions developed during this study. This enabled a comparison of the past modeling results with those generated during this round of model development and calibration.

1.3.4 New Data Added Since Previous Work

New water level and permeability information were added in order to support the discretization of boundary conditions and permeability information. Sections 2.3 and 2.4 of this report provide more detail relating to the locations of these wells and the new data gathered.

1.3.5 Coupling of Vadose Zone and Aquifer Model Domains

The local grid refinement capability of TETRAD allowed a portion of the aquifer model horizontal domain to match the footprint of the SDA vadose zone model domain. This enabled the 1:1 match of the horizontal domains within the refined area of the saturated zone model. Mass flux of water (and contaminants, even though their presence is not discussed in this report) leaving the base of the vadose zone model at specific times could be input to the aquifer model using "MFLUX" or "MFLUXT" cards in a TETRAD data deck.

1.3.6 Flow Model Calibration Overview

Simulated hydraulic heads were compared with values measured in the southern INEEL. First, an attempt was made to qualitatively reproduce water level trends observed in water table maps created during the data evaluation phase of this study. In past aquifer flow model calibration efforts (Magnuson and Sondrup, 1998), only this qualitative level of calibration was performed.

In order to measure the level of accuracy of the model quantitatively, model residuals were calculated using water levels measured in each of the wells contained in the aquifer model domain. Root mean square error (RMS), mean absolute error (MAE), and mean error (ME) were calculated from the model residuals. Parameters were adjusted by trial and error in an effort to minimize errors in simulated head values.

1.3.6.1 Qualitative Goals

In order to create an aquifer flow model that is representative of field conditions near the SDA, the following qualitative goals were considered during model development:

- General trends observed in water table maps of the area should be reproduced in the flow model.

- Where point (i.e. well) measurements of hydraulic parameters are averaged to produce "blocks" with average hydraulic properties, each of the point locations should be contained in the blocks in which their values were assigned.

1.3.6.2 Quantitative Goals

The following goals were developed in order to assess the quality of this model with respect to previous modeling efforts:

- The quantitative fit (as measured using RMS, MAE, and ME) of the "best" model produced during this effort should be better than the fit of an approximation of one of the best previous cases over the entire model domain.

- The quantitative fit in the immediate vicinity of the SDA should be better than (or, at least, approximate) the fit of an approximation of the best previous run.

- The RMS will be used as the primarily calibration measure because it is most helpful in identifying gross simulation errors. MAE and ME will be used as secondary and tertiary measures, respectively.

2. AQUIFER MODEL DEVELOPMENT

This section presents the development and implementation of the simulator to describe the movement of water in the aquifer beneath the SDA. One note of caution is in order. Because the TETRAD simulator uses metric units, meters are used in much of the discussion and graphical portrayal of model results. However, in some cases, particularly when referring to water level measurements, feet are used since it is common practice at the INEEL to discuss depths in terms of feet.

2.1 Conceptual Model

The subsurface at the SDA is comprised of fractured basalts occasionally interrupted by thinner sedimentary layers ("interbeds"). Water flow in the fractured basalts is considered to be primarily controlled by the fractured network. Magnuson (1995) found that a single-porosity system representing only the fractures could reasonably explain existing hydrologic data as long as gas-phase flow was insignificant. As such, in water-saturated groundwater models produced in the past (Magnuson and Sondrup, 1998) and during this study, the basalt aquifer has been modeled as a single high permeability, low porosity medium. Permeability is spatially variable within the basalt aquifer as indicated in pump test results and as possibly implied by a non-uniform hydraulic gradient in the southern INEEL (although it is recognized that other factors, including enhanced ground water recharge in certain areas, could also contribute to the heterogeneity of the hydraulic gradient).

2.2 Model Domain and Discretization

The selection of the model domain was guided in part by several factors including;

- The desire to maintain consistency with past groundwater flow modeling efforts;

- The steady-state distribution of water levels near the SDA as observed during several water level measurement periods;

- A requirement that risk concentrations be estimated for contaminants at the INEEL's southern boundary (Magnuson and Sondrup, 1998); and,

- The desire to include several new wells in the interior of the model domain.

Figure 2-1 shows deviation corrected water levels measured during March/Early April and October/Early November of 2000 along with the base grid used during this study. A more thorough discussion of the water level data used to produce these maps will be included in section 2.3. Other seasonal water level information was collected and mapped. Those data are not portrayed here owing to their similarity to the spring and fall 2000 water level maps (Figure 2-1).

The horizontal model domain selected for this effort is similar in dimensions to (although slightly larger than) the domain selected during the most recent round of modeling (Magnuson and Sondrup, 1998). Aside from the similarity in size to the previous domain, it was selected based on the fact that water level patterns observed at the edges of the domain are consistent over both the March/April and October/November time periods (and two other time intervals that are not shown here) in 2000. This was an assumed indication that the edges of the model domain were at steady state whereas some variability in water level patterns in the interior of the domain might be explained by sources or sinks in the interior of the discretized area (i.e., wells, recharge zones, etc.) and/or a slightly different suite of wells used to produce the water table maps. The domain was also chosen so that it contained several new wells north of the RWMC as well as the INEEL's southern boundary.

The base grid is divided into 304.8 m x 304.8 m (1000 ft x1000 ft) grid cells situated in 27 rows and 34 columns in the horizontal plane (a total of 918 grid cells per each horizontal layer). The base grid is divided into 7 layers in the vertical direction. The thickness of the domain is 76 m (250 ft) and is consistent with Magnuson and Sondrup (1998). The domain is discretized entirely as the ESRPA aquifer with none of the horizontal layers representing the vadose zone beneath the SDA. The horizontal origin of the base grid is (249500 ft E, 650500 ft N).

In order to ensure a 1:1 match of a portion of the aquifer domain with the current vadose zone model domain, one refined area was added in the SDA area with its origin located at (263500 ft E, 666500 ft N). The grid cell size in the refined area is 152.4 m x 152.4 m (500 ft x 500 ft) in the horizontal plane. The grid was left unrefined in the vertical direction. A total of 140 grid cells compose each horizontal layer of the refined area. Figure 2-2 superimposes the refined area on the base grid.

2.3 Aquifer Boundary Conditions

Constant head boundaries were assigned at the perimeter of the model domain based on the water table map generated from March/Early April measurements (Figure 2-1). The asterisks evident in Figure 2-1 represent the grid locations at which water level data were applied to the first layer of the aquifer model. Water pressure (as a surrogate for hydraulic head) is input to TETRAD in units of kg/m^2. A water pressure gradient of 111.13 kPa/m was used in order to apply boundary conditions to the perimeter of horizontal layers beneath the top layer.

Most of the data used to produce the water table maps were previously corrected for deviation from vertical and were requested and delivered directly from the HDR database. New wells listed in the HDR database that were used during this study that were not used during the previous round of modeling include USGS-OBS-A-125, CFA-MON-A-001, CFA-MON-A-002, and CFA-MON-A-003. With the exception of USGS-OBS-A-125, none of the new wells from the HDR database are located within 1000 m of the selected model domain.

A deviation correction for the new wells listed in the HDR database was indicated as 0 ft. For the sake of this study, it was assumed that data originating from the HDR database were deviation corrected if deviation logs exist for the wells in question. However, it is unclear whether gyroscopic deviation logging was performed for these wells and the vertical correction is nil or whether "0 ft" is indicated in the database where no deviation data exist.

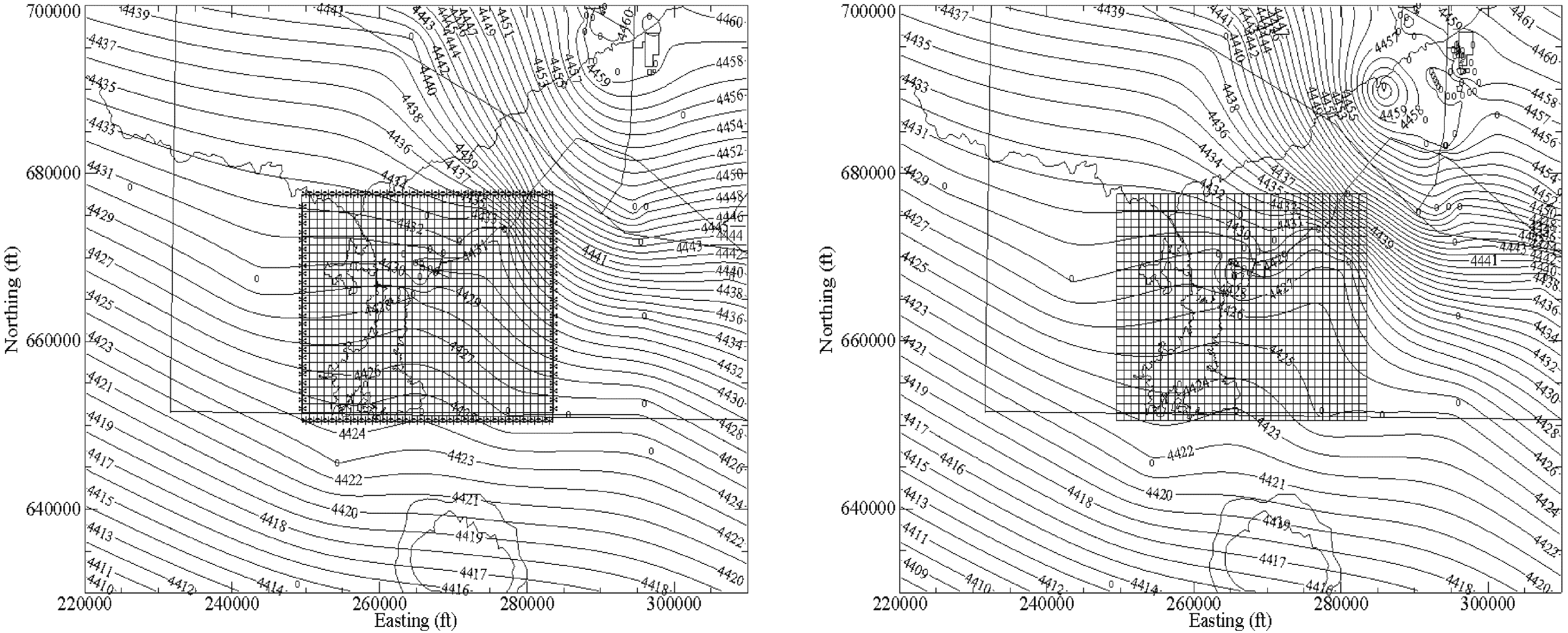

Figure 2-1. Water table maps generated with deviation-corrected data gathered for March/April (A.) and October/November (B.) 2000. The horizontal modeling domain is shown on both maps. The asterisks along the domain perimeter in (A.) are locations at which heads were input to TETRAD for boundary conditions.

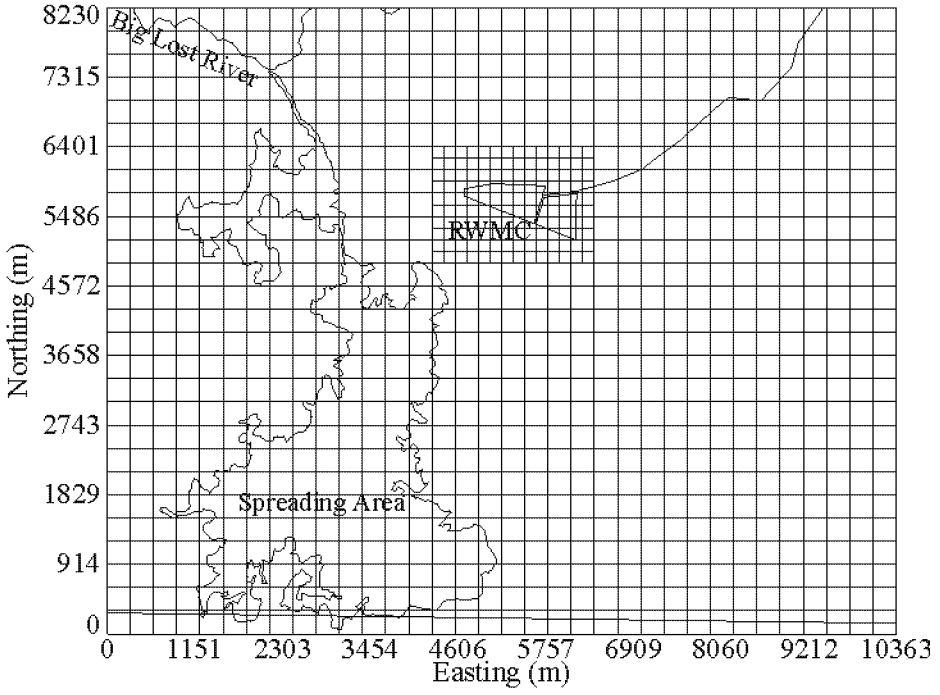

Figure 2-2. Map of the base domain and refined area (in meters).

Data input from gyroscopic deviation information are input to Century Geophysical, Inc. processing software to generate corrected well depths at specific measured depths in each well. Corrected water levels are calculated using the equations below:

$$Diff_d = TDepth_d - Depth_d \quad (1)$$

$$Corhead = Head_d - Diff_d \quad (2)$$

where the subscript *d* refers to the depth at which the water level is measured in a well, *Depth* is the measured depth to water, and *Tdepth* is the "true" depth to water calculated

from deviation information supplied to the Century Geophysical software. *Corhead* is the corrected head (or, water table elevation since mean sea level is the datum used during this study) at the well.

Aside from the new water level data supplied by the HDR, water level information from M11S, M12S, M13S, M14S, and USGS-127 were gathered independently from recent field logs[1]. Except for USGS-127, all of these wells are located in the northern portion of the model domain and help define water level trends north of the SDA. USGS-127 is located east of the model domain near the CFA and supports the steepened hydraulic gradient south and southwest of INTEC (see Figure 2-1). Borehole deviation logs were collected for each of these wells and corrections were applied using equations (1) and (2).

Two other wells for which water level data were available were excluded from the water table maps produced during this study: A11A31 and USGS-088. Both wells are located south of the RWMC. The elevation of the surface measurement point (stickup) is questionable for A11A31. At least 2 stickup heights have been reported with one being approximately 1 ft above ground surface and the other being approximately 3 ft above ground surface[2]. A new stickup measurement is required before this well can be used again for production of water table maps in the area.

USGS-088 was excluded because it has been hypothesized that the well taps an isolated zone in the ESRPA and that water levels may be heavily affected by standing water in the spreading areas southwest of the RWMC (Wood, 1989). Water was not added to the spreading areas in 2000; however, water has been added as recently as 1998. While USGS-088 water levels did not appear to be anomalous when compared to its nearest neighbors during 2000, it was excluded since it may or may not be representative of conditions in the aquifer surrounding.

Well M4D remains in the data set despite its closeness to USGS-088 and its relatively high water level compared to adjacent wells. No published report has discussed the potential anomalous behavior of water levels in M4D; therefore, water level information from the well was retained for this study. Because water level data from M4D might not be representative of the aquifer surrounding it, quantitative measures of aquifer model calibration will be supplied for cases in which the well is both excluded and included in the data set. Figure 2-2 is a map of the wells that were either newly added or excluded from this study.

---

[1] Data gathered by Terri Bukowski (BBWI), January 2001.

[2] Personal communication with Ron Arnett (BBWI), March 2001.

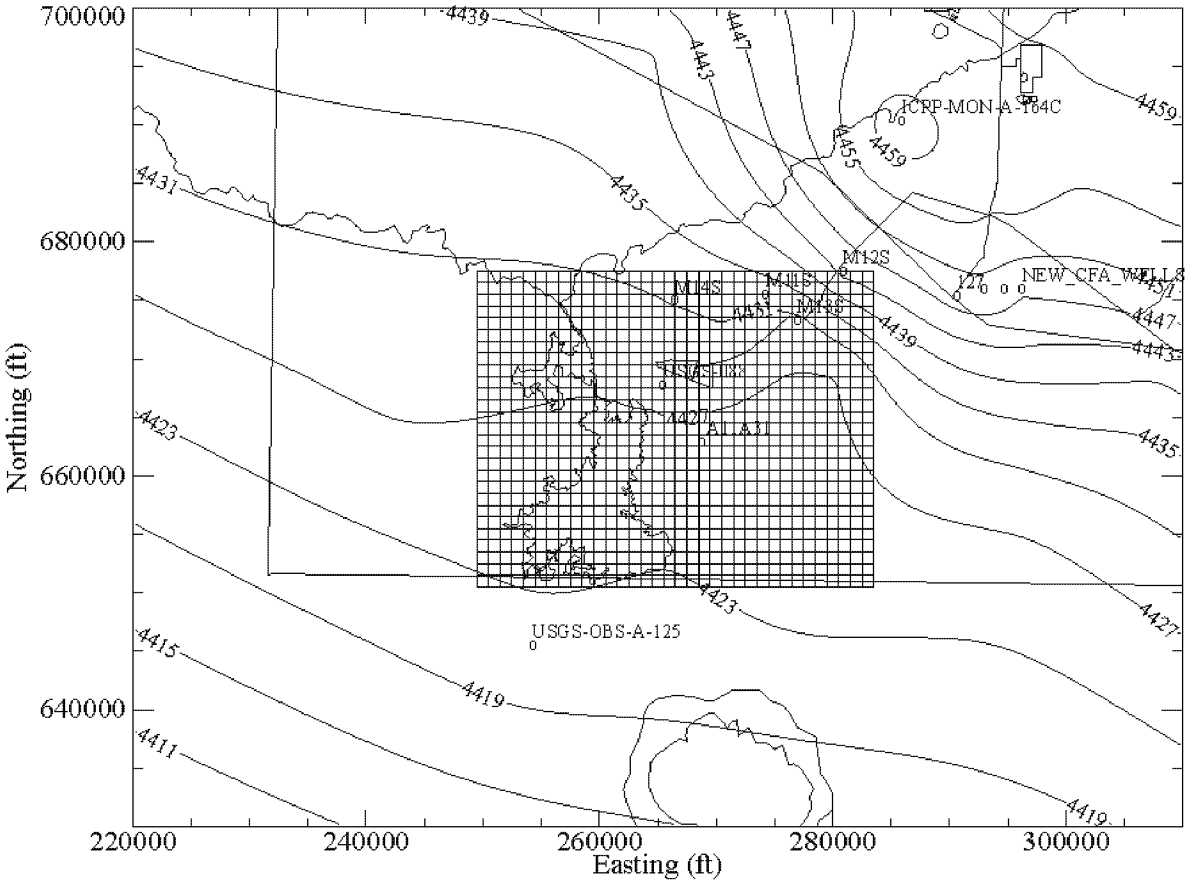

Figure 2-2. Map of wells newly added or excluded from the water level dataset for the modeling study.

2.4 Hydrologic Properties

ESRPA permeabilities were calculated from existing transmissivity data from both pumping tests and specific capacity information for 21 wells located inside the model domain (Ackermann, 1991; Wylie and Hubbell, 1994; Wylie 1996). Table 2-1 lists the permeability data used during this study. Figure 2-3 shows the location of the wells from which permeability data were gathered.

Table 2-1 shows the permeability information divided into 3 classes. Wells contained in the low permeability class (153 mD) are situated immediately south of the SDA. The middle permeability class (9300 mD) is composed of wells located north and northwest of the SDA. Finally, the high permeability class (712000 mD) consists of wells located generally south and east of the SDA.

Magnuson and Sondrup (1998) computed 3 similar permeability classes averaging 153 mD, 10660 mD, and 1200000 mD, respectively. Their middle and high permeability classes were calculated using fewer data points than were used here. Retention of each of the wells used to calculate permeability averages in their appropriate permeability zones was not considered a priority during that study; therefore, some of the wells used to calculate the low classification mean permeability were not (spatially) included in the low permeability zone.

As discussed in section 2.1, the aquifer can be modeled as a high permeability, low porosity medium representing only fractures. Therefore, a porosity of 0.062 is used for the entire aquifer in this study and is consistent with the previous modeling effort (Magnuson and Sondrup, 1998).

Table 2-1. Permeability data used during the aquifer modeling study.

Well	Transmissivity (ft^2/d)	Thickness of Sat./Open Interval (ft)	Permeability (mD)	Mean Perm. (mD)
M10S	5	30	49	
USGS-88	13	87	55	
USGS-89	49	56	319	
USGS-117	14	74	69	153
USGS-119	1.1	105	4	
M1SA	20	30	243	
M4D	4	30	61	
M6S	30	26	421	
EBR-I	1300	479	990	
USGS-86	300	46	2380	
USGS-87	850	87	3570	
USGS-90	490	31	5770	9300
Pit9	1000	40	9120	
M3S	1000	30	12170	
M7S	1000	30	12170	
RWMC-Production	6800	112	21590	
USGS-106	100000	177	206060	
USGS-109	110000	182	220400	
USGS-120	220000	94	854500	712000
USGS-9	59000	28	768500	
LESAT	1000000	250	1508700	

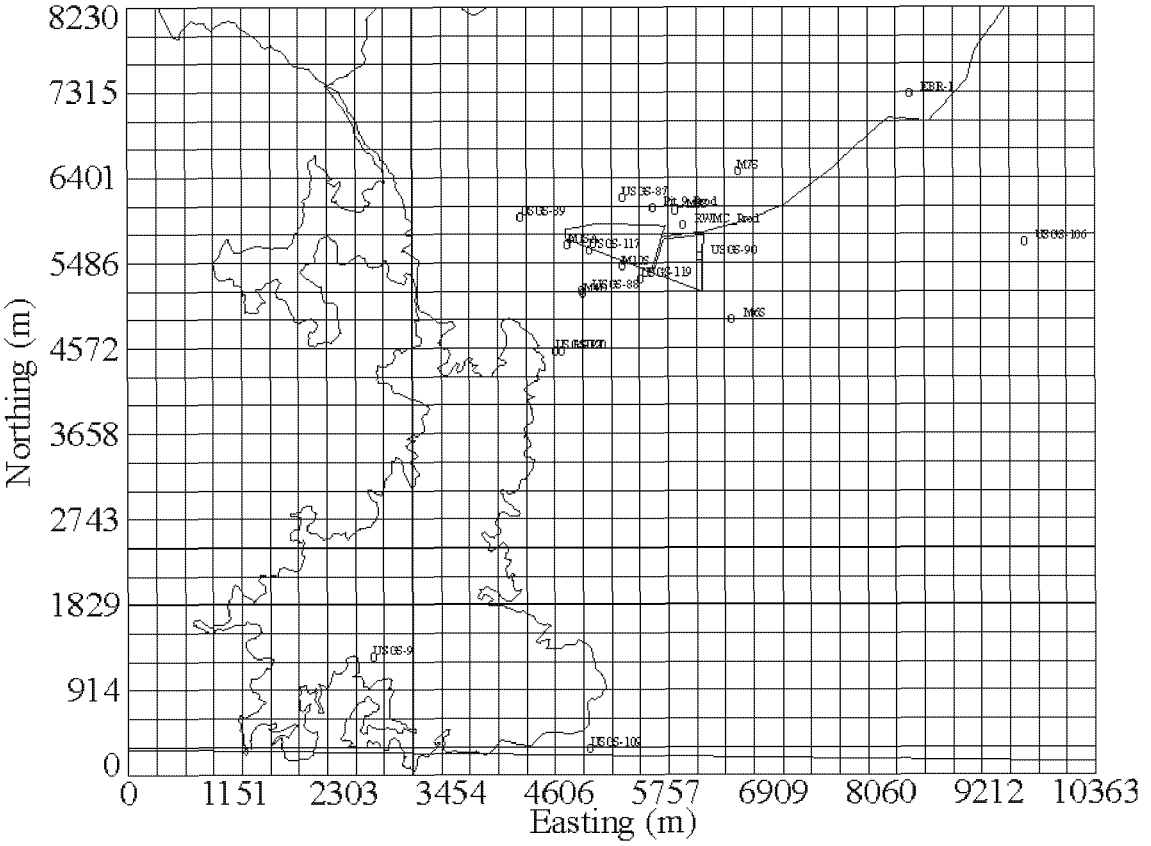

Figure 2-3. Map of wells used to calculate aquifer permeability regions.

2.5 Summary of Model Assumptions

The following list contains the assumptions used in developing the groundwater flow model:

- Water levels measured as much as 1.5 months apart are adequate for producing accurate water level maps.
- Vertical flow gradient effects are insignificant in the aquifer (i.e., water levels measured in wells with different screened intervals are comparable).
- Different measuring devices (i.e., steel vs. plastic measuring tapes) produce no differences in measured water levels.
- Pump tests performed over different depth intervals produce transmissivity and permeability estimates that are representative of the entire aquifer thickness at a particular location (i.e., no vertical variation in permeability).

- USGS-88 is invalid for water level maps because it is hydraulically isolated.

- Wells used to calculate the average permeability of a spatial permeability zone should be included in that permeability zone.

- Over a majority of the model domain, aquifer permeability is high enough and mass flux from the vadose zone in low enough that water levels in the aquifer are unaffected by infiltration; therefore, it is only necessary to add mass flux of water to the aquifer in the refined area since that area contains the only low permeability zone in the model domain.

- The screened interval of pump tested wells is equal to b where Transmissivity = (Hydraulic Conductivity) x b, regardless of the actual effective thickness of the aquifer at any location (i.e., partial penetration effects are ignored).

- Lithology is uniform over the entire depth of the aquifer.

- The beginning date of simulations produced during this study is 1/1/52.

- The aquifer can be represented by a single high permeability, low porosity medium that represents only the fracture system in the aquifer.

- Water levels in the aquifer are at steady state.

- Deviation corrected water levels are accurate and can be used to produce steady state water table maps.

- The effective thickness of the ESRPA is 76 m.

- A low permeability zone exists beneath and immediately southwest of as depicted in Wylie (1996).

- Constant head boundary cells are unaffected by the addition of water to the spreading areas (the validity of this assumption is discussed in sections 3.4 and 4.3).

- The mass flux output from the recent vadose zone model accurately reflects field conditions (Note - the aquifer model is calibrated with the mass flux from the vadose zone model added).

2.6 Coupling of Mass Flux Data from the Vadose Zone

A PV-WAVE program was written that produces "MFLUXT" and "MFREG" cards from vadose zone model output recently generated by Swen Magnuson (BBWI)[3]. The

[3] Coincident with this study, Mr. Magnuson developed a simulator for vadose zone transport as a refinement of the work presented in Magnuson and Sondrup (1998).

vadose zone output file used as input to aquifer model was tr3.1.GV.BIN. Mass flux in TETRAD is input in units of $(kg/m^2)/d$. The PV-WAVE program was checked to ensure that water from the vadose zone was applied only to the top layer of the refined area (140 cells total).

3. AQUIFER FLOW MODEL CALIBRATION

This section is divided into four main sections: one outlining the results of simulation discretized as an approximation to past work, the second describing the results of a model run produced using kriged permeability data, the third summarizing the best case generated in this round of modeling, and a fourth showing the effects of the addition of infiltration to the spreading areas during the 1982 to 1985 time period. Aquifer boundary conditions and grid geometry remain constant throughout each of the conditions discussed below.

3.1 Approximation of Previous Work

Figure 3-1 is a map of the permeability distribution used to approximate Case 3 developed in the previous round of groundwater flow modeling. While a minor alteration to Case 3 (Case 4) was considered the "best" case by Magnuson and Sondrup (1998), Case 3 is presented here owing to its similarity to this model with respect the assumed aquifer thickness. The "FTOPS" module of TETRAD was used during case 4 to vary the aquifer thickness inside the model domain. Qualitatively, Case 4 was, at best, marginally better than Case 3. No quantitative measures of fit were used during the previous simulation effort.

Figure 3-2 presents results and quantitative measures of fit for the Magnuson and Sondrup (1998) Case 3 approximation. In general, simulated water level trends match measured water levels to the extent that inferred groundwater flow direction is to the south and southwest and the hydraulic gradient is generally lower in the southern portion of the domain than the northern portion. The southward inflection of water table contour lines in the vicinity of the RWMC is evident in both the simulated and observed maps (see Figure 2-1).

Quantitative measures of fit are RMS = 1.566, MAE = 1.075, and ME = -0.635 where the statistics are calculated as follows:

$$RMS = \sqrt{\frac{\sum_{i=1}^{n} (\mathrm{Re}siduals)_i^2}{n}} \qquad (3)$$

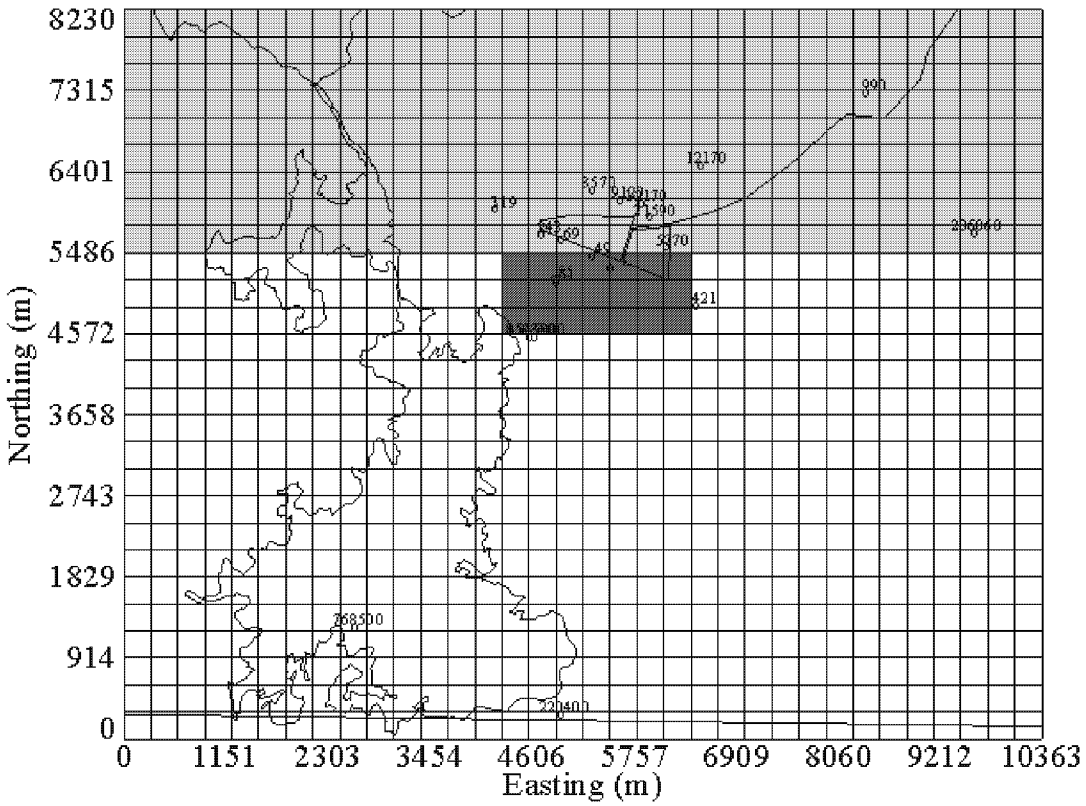
8230
7315
6401
5486
4572
3658
2743
1829
914
0
Northing (m)
0
1151
2303
3454
4606
5757
6909
8060
9212
10363
Easting (m)

Figure 3-1. Map of the permeability distribution used to approximate Magnuson and Sondrup (1998) Case 3. The grid is discretized as follows: white = 1200000 mD, light gray = 10660 mD, and dark gray = 153 mD. Permeability values calculated from pump-test transmissivity data are included for reference.

$$MAE = \frac{\sum_{i=1}^{n} |\mathrm{Re}siduals|_i}{n} \tag{4}$$

$$ME = \frac{\sum_{i=1}^{n} (\mathrm{Re}siduals)_i}{n} \tag{5}$$

where n is the number of wells inside the model domain (or portion of the domain in the case of the refined area) at which measured water levels can be compared with simulated

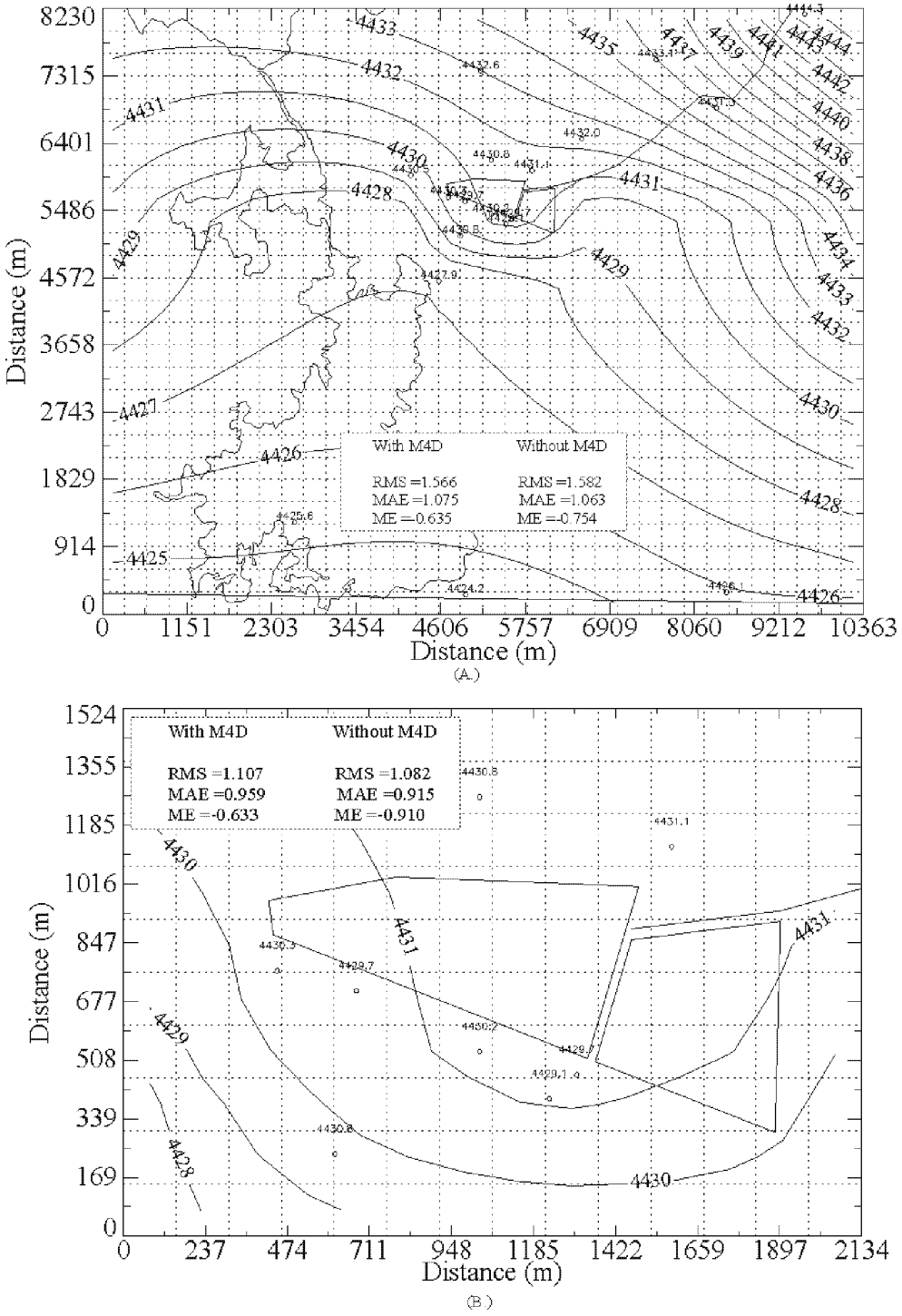

Figure 3-2. Simulated hydraulic heads for the approximation of Magnuson and Sondrup Case 3. Quantitative measures of calibration fit are included for both the entire domain (A.) and refined area (B.). Heads and measures of fit are in feet.

heads. Residuals were calculated by importing the grid files (*.GV) generated in TETRAD to Surfer. The output generated by TETRAD is in pressure units. The pressure units are easily converted to units of head using Surfer's "Grid/Math" function. Using Surfer's "Grid/Residuals" function, the difference is calculated between the converted grid and the values measured for March/April. Surfer uses linear interpolation between grid nodes (Surfer uses a mesh-centered gridding approach) to estimate simulated heads for well locations not located directly at TETRAD simulation nodes.

3.2 Geospatial Distribution of Permeability

Since pump-test derived aquifer transmissivity estimates have been published for numerous wells at the INEEL (Ackermann, 1991), one goal of this study was to geostatistically simulate the spatial distribution of aquifer permeability. For the 21 wells located in the model domain for which pump-test data exist, a relatively poor spatial correlation structure with range = 1800 ft, sill = 13, and nugget = 0 for the natural log of permeability was found with very few data pairs. Figure 3-3 is map of the (back-transformed) permeability distribution input to TETRAD created using universal kriging and the spatial correlation parameters mentioned above.

Figure 3-4 is a map of hydraulic head simulated with the permeability distribution shown in Figure 3-3. On both a quantitative and qualitative basis, the results are a poor reproduction of observed heads. A large groundwater mound is produced immediately south of the RWMC owing to the very low permeability geostatistically simulated for that location and the flux of water input from the vadose zone. That groundwater mound is not observed in field measurements of water levels in nearby wells. As a result, this run is considered an inadequate simulator of groundwater flow inside the model domain.

3.3 Best Model Case

After numerous attempts to minimize errors while adhering to the study guidelines listed in section 1.3.2 of this report, the permeability scenario depicted in Figure 3-5 was produced. With exception of well M6S, all wells used to calculate the average permeability for each of the permeability zones are contained in the appropriate zone. Well M6S (421 mD) is situated immediately outside the 153 mD permeability zone that it was used to calculate.

The permeability boundary between the high and middle permeability zones in the northwest portion of the domain approximates the boundary used during groundwater modeling performed for WAG-10 (Magnuson and Sondrup, 1998 (Case 1)). The distribution of permeability shown in Figure 3-5 is unique in that it was calculated with data not used during previous studies; therefore, permeability values and the geometry of the permeability zones are different from those used during previous efforts.

Figure 3-6 presents the results of the simulation run using the permeability configuration presented in Figure 3-5. Qualitatively, general trends observed in the March/April water level data are produced in this run. Inferred groundwater flow direction is to the south and southwest and the inflection in isolines near the RWMC is produced. Quantitatively, each of the measures of fit are less for this scenario than those calculated for

the approximation of Magnuson and Sondrup Case 3 over the scale of the entire model domain. The quantitative measures of fit for this case are similar to (but marginally worse than) the Case 3 results inside the refined area. The isoline pattern in the northwest portion of the model domain is more accurately produced with this simulation than with Case 3.

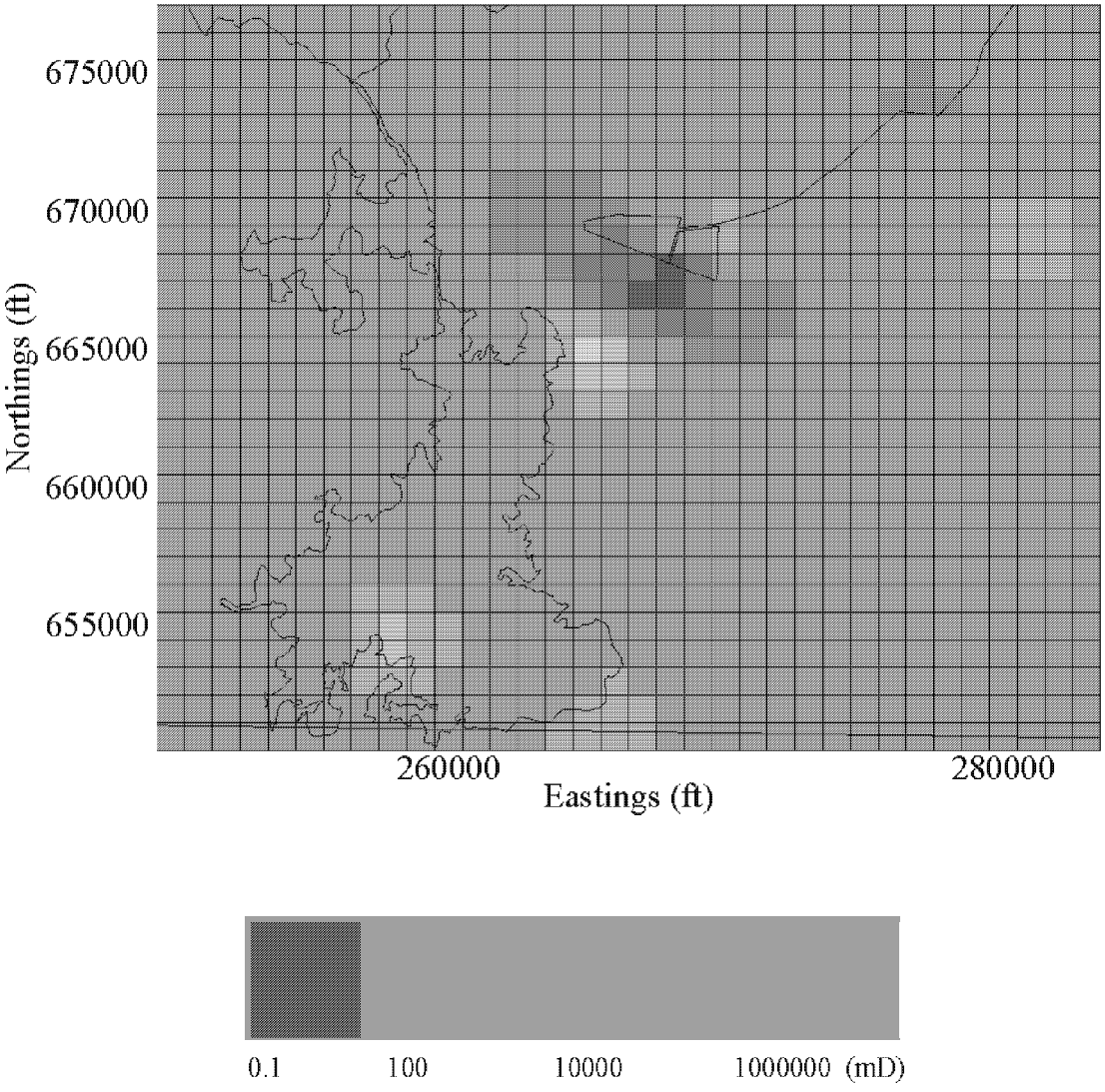

Figure 3-3. Kriged permeability distribution input to TETRAD. This geostatistical representation identifies the low and high permeability regions observed in pump-test data;

however, permeability is somewhat "bulleted" owing to the short spatial correlation range observed for the data (1800 ft).

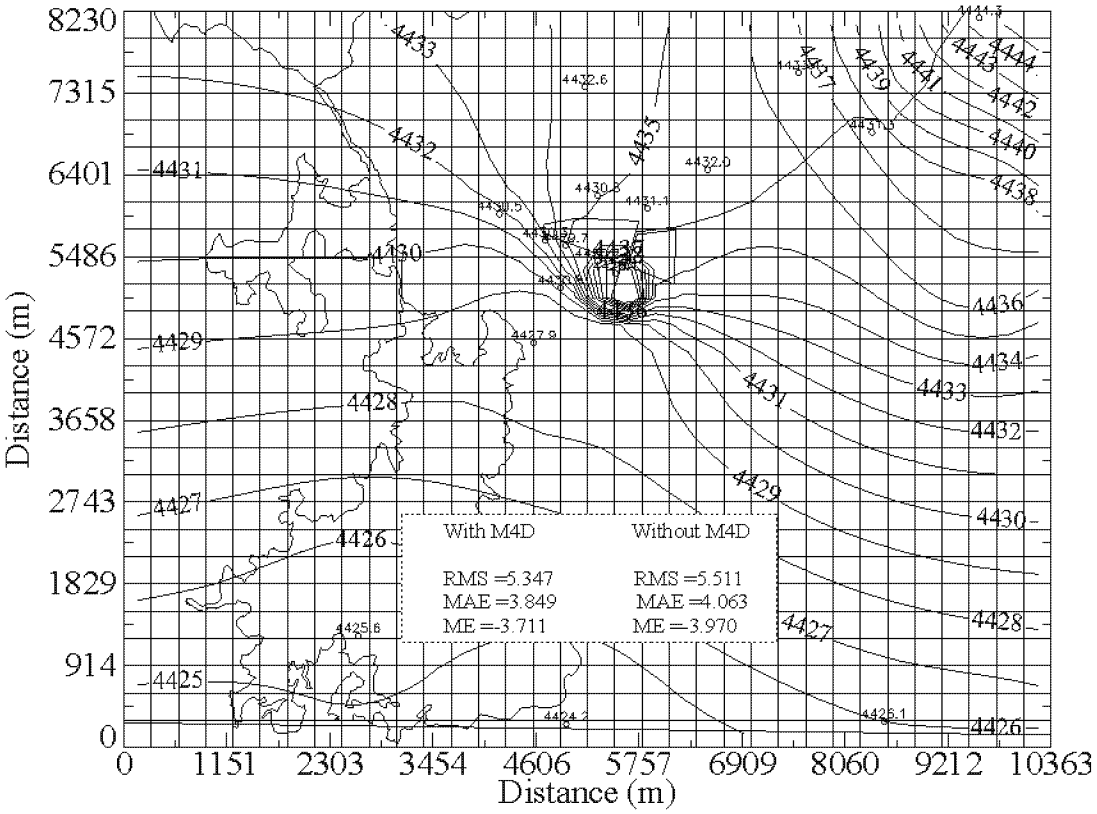

Figure 3-4. Map of simulated heads for case where geospatially analyzed data were input to the TETRAD data deck.

This case produced the best results during this modeling study as measured by quantitative fit over the model domain. Additional enhancements of this simulation over Magnuson and Sondrup Case 3 are the augmentation of the permeability dataset and the retention of wells in the permeability zones in which they were used to calculate average values. Finally, general water level trends observed in water table maps generated with deviation-corrected water level data are reproduced in this simulation scenario.

3.4 Addition of Water to Spreading Areas A and B

In order to assess the influence of the spreading areas on groundwater flow near the RWMC, two infiltration scenarios were input to the best simulation case. Infiltration rates were estimated for the time period from November, 1982 to June, 1985 during which water was added to spreading areas A and B from the Big Lost River. Volumetric infiltration rates were calculated as the total volume of water discharged to each basin divided by 950

days (11/30/82 to 6/30/85). One-dimensional infiltration rates were calculated for 2 different scenarios by dividing the volumetric infiltration rate by the area into which the water was infiltrated. Figure 3-7 shows the two spatial scenarios that were used to simulate spreading area infiltration.

During the first case, the water was infiltrated into an area of 1496000 m^2 in spreading area A and 2900000 m^2 to area B. TETRAD requires mass flux input (rather than infiltration rate input). The resultant mass flux input for this "large" spatial case was 91 $kg/m^2/d$ to A and 185 $kg/m^2/d$ to B.

During the second case, the water was infiltrated to 465000 m^2 and 557400 m^2 in areas A and B, respectively. The corresponding mass flux rates are 290 $kg/m^2/d$ and 965 $kg/m^2/d$.

Figure 3-8 consists of maps of each of the infiltration cases discussed above. In both cases, the subtle groundwater trough centered at near USGS-120 in Figure 3-5 has shifted eastward. Both cases suggest that a southeastward groundwater flow direction could develop immediately south of the RWMC if water is added to the spreading areas.

The accuracy with the best-case simulation reproduces heads observed during the 1982 to 1985 time period is beyond the scope of this study. However, a qualitative discussion of the sensitivity of the model to spreading area infiltration is provided in section 4.3 of this report.

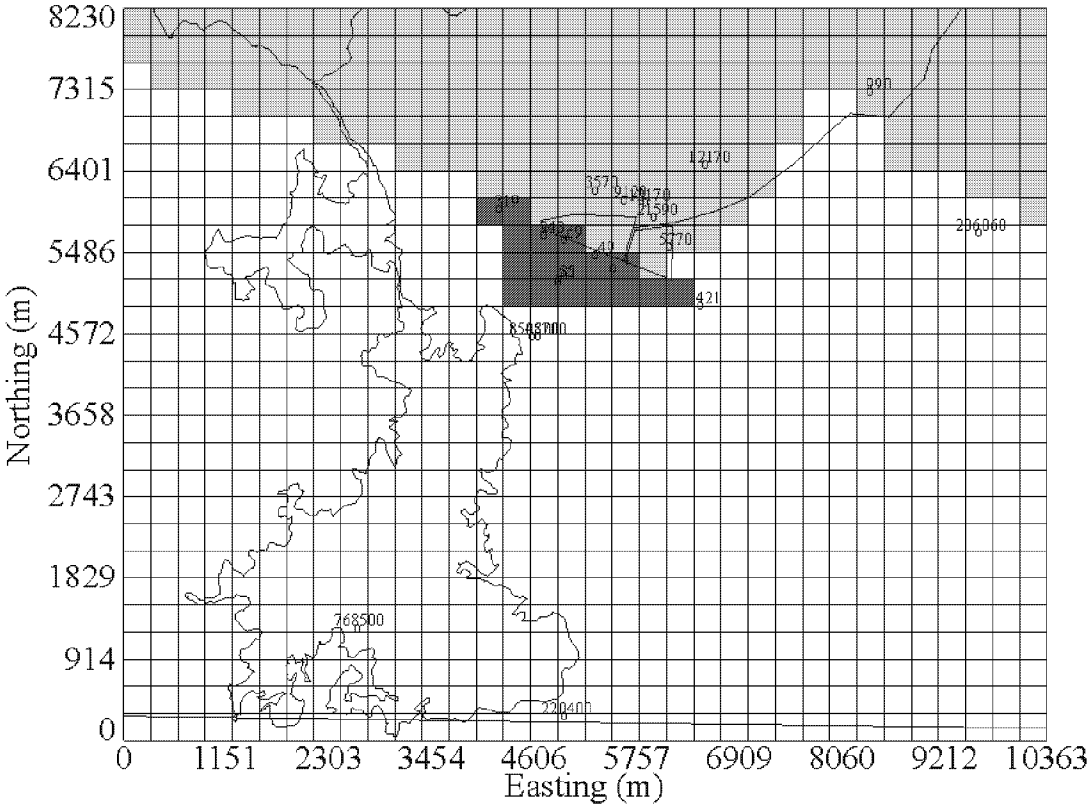

Figure 3-5. Permeability distribution used during the simulated best case. White = 712000 mD, light gray = 9300 mD, and dark gray = 153 mD.

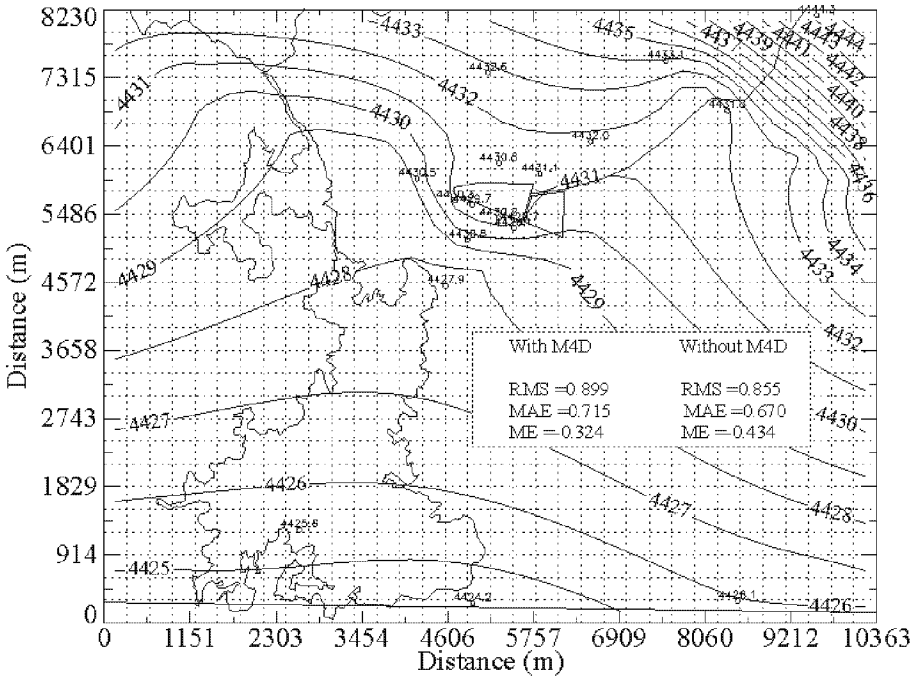

(A.)

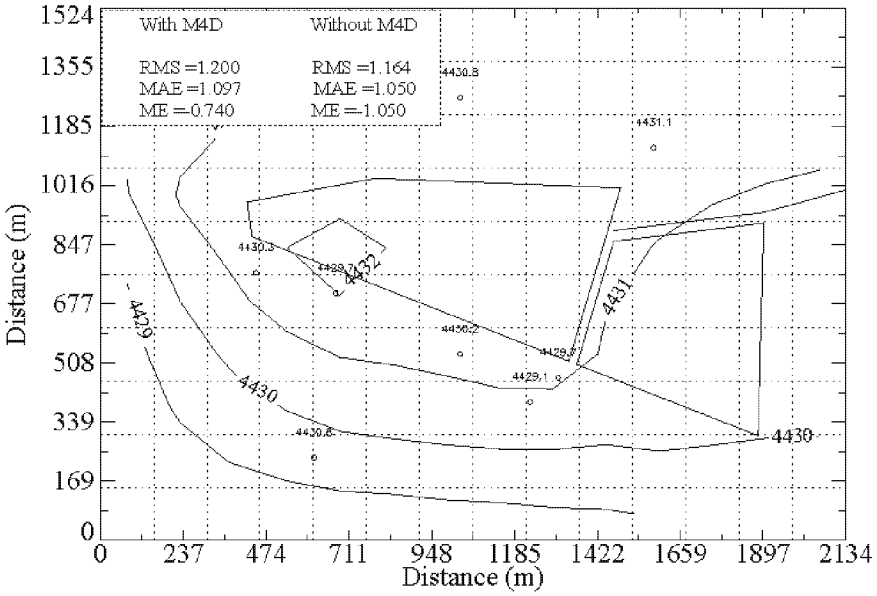

(B.)

Figure 3-6. Simulated heads produced with the permeability configuration depicted in Figure 3-5.

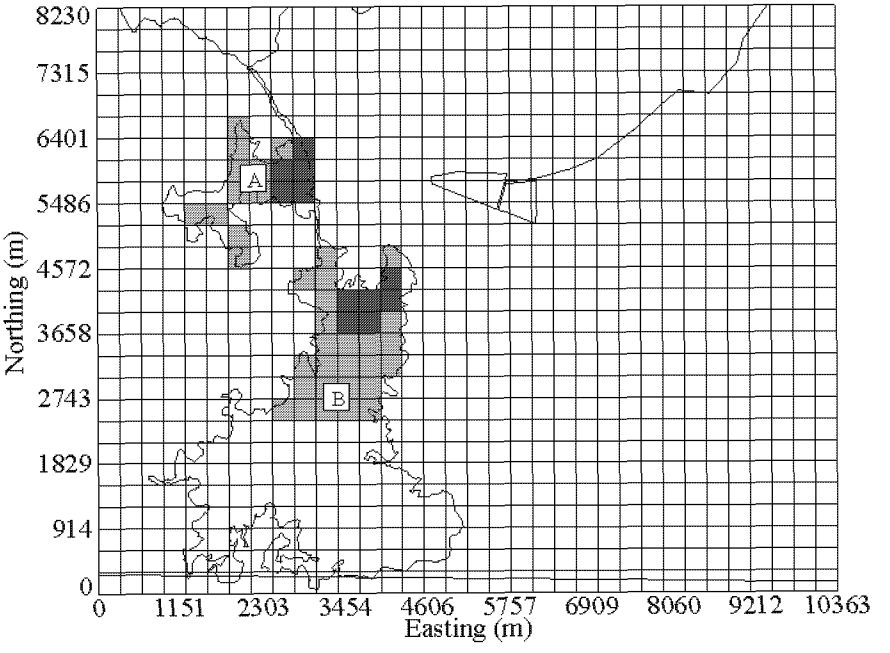

Figure 3-6. Map of the two areas discretized to include spreading area infiltration.

4. DISCUSSION

The current study yielded results that were consistent with the guidelines, objectives, and goals of this study in that:

- New data were used in the development of the best-case model;
- The model developed during this study can be coupled with output from a model of vadose zone water and contaminant transport;
- Water level information from two wells were excluded from this study based on uncertainties regarding the representativeness of the recorded water levels in the HDR database;

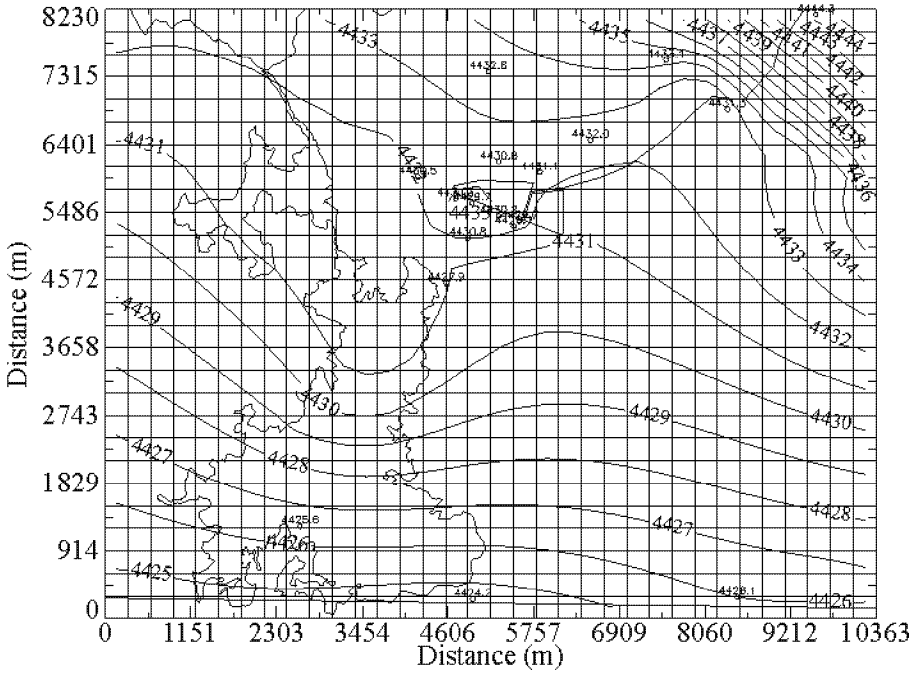

(A.)

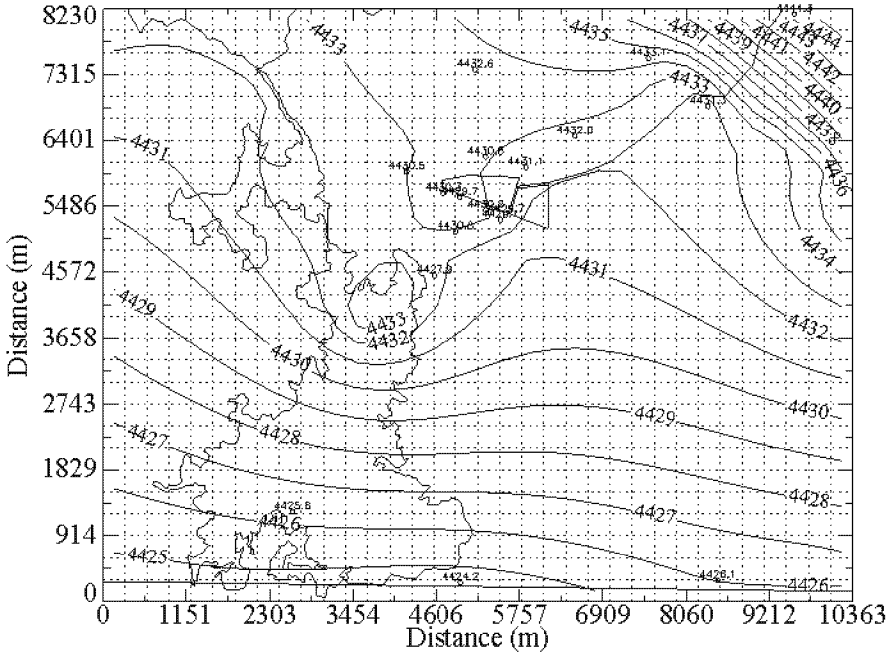

(B.)

Figure 3-7. Maps of simulated hydraulic head for the large (A.) and small (B.) spatial additions of infiltrating water to the spreading areas at 12000 days (from 1/1/52).

- The best-case simulation produced during this study is more accurate, as measured by quantitative fitting parameters, than an approximation of one of the best previous cases;

- The best-case simulation maintains consistency with past model geometries where prudent;

- Geostatistically analyzed permeability data were included in one run; however, inaccurate results were produced during that run; and,

- Point measurements used to calculate average zones of permeability are included in the appropriate permeability zone with only one minor exception.

A more detailed discussion of the best-case simulation, the model accuracy, model sensitivity, and suggestions for future work is included below.

4.1 Best Simulation

The best-case run developed during this study is an improvement over a best previous run based on its quantitative fit to measured water levels. Further comfort can be taken in the fact that wells from which permeability information was used to calculate zones of average permeability are included the appropriate zones.

The addition of more wells to the permeability data set also helps to support the validity of the flow model. Because the flow model is bounded on all sides by constant head boundaries, a large number of permeability values could fill the "middle" and "high" permeability classifications depicted in Figure 3-4 to produce a nearly identical distribution of simulated heads in the absence of stresses to the aquifer (i.e., recharge, pumping wells, etc.). The only factor required to produce a similar distribution (again, in the absence of stresses) would be that the ratio of the "middle" to the "high" permeability classes is the same and the geometry of the permeability zones were the same. So, it is valuable to include as much data as possible in the permeability data set in order to constrain the discretization of the "middle" and "high" permeability classes.

4.2 Accuracy of the Flow Model

The accuracy of the flow model can be quantified by the RMS. Because the RMS is identical to the standard deviation of the error residuals, the best-case RMS of 0.899 ft (1σ) means that there is a 95% probability that each of the observed water levels is simulated to within 1.8 ft (2σ) accuracy, if the residuals are normally distributed. Of course, very few data points (17 wells) were used for the calibration; therefore, the normality of the residuals cannot be proven. Nonetheless, the RMS can be used as a general guideline to show that the best-case simulatio reproduces observed heads to within 2 ft at most locations.

4.3 Discussion of Model Sensitivity

A thorough discussion of model sensitivity is beyond the scope of this study. However, some semi-quantitative and qualitative comments might be of interest to other parties seeking to assess the influence of the spreading areas (and groundwater recharge in general) on the aquifer.

A very limited water level dataset (7 wells) was gathered for the 1982 to 1985 time period. Among those wells expected to be influenced by the addition of water to the spreading areas during that time period, USGS-89 showed a water level increase of approximately 20 ft from January, 1982 to October, 1984. While this might initially infer that the spreading areas have a dramatic effect on water levels near the RWMC, it is necessary to determine whether or not a regional water table rise may have also contributed to the water level rise.

Water levels at USGS-8, USGS-103, and USGS-22 rose by approximately 12.5 ft, 8.5 ft, and 10 ft, respectively, during the 1982 to 1985 time period. Each of these wells are located several miles from the spreading areas and outside the model domain used during this study. This relatively large water level rise in wells, which are unlikely to be affected by the spreading areas, infers that a significant portion of the water level rise at USGS-89 may result from a regional water table rise as opposed to merely addition of water to the spreading areas.

Compared to simulated best-case heads generated without spreading area infiltration, the "small" spatial addition of water to the spreading areas resulted in a simulated head increase of approximately 2.5 ft at USGS-89 (Figures 3-4 and 3-7(B.)). Assuming the regional water level rise and spreading area infiltration were the only factors contributing to water level rise at USGS-89, approximately 8.5 ft to 12.5 ft of the increase is attributable to the regional water table rise based on the three "background" wells listed above. Therefore, a 7.5 ft to 11.5 ft increase in water levels could be attributed to the addition of water to the spreading areas. The best-case simulation including the small area, high flux spreading zone infiltration scenario causes a water level rise at USGS-89 of only 22% to 33% (2.5 ft) of the observed water level rise (7.5 ft to 11.5 ft), if the assumptions listed here are correct.

It is unclear whether the model does not match observed heads due to errors in permeability parameterization or due to uncertainties in discretization of spreading area infiltration. Some uncertainty exists regarding the surface area of the spreading basins submerged beneath standing water during time periods when water is added to the ponds. Further, no pump test data is available from any wells located in or directly adjacent to spreading area A. Both of these factors could contribute to the difference between the observed and simulated heads. However, both simulated and observed heads show that a southeastward groundwater flow direction can be inferred upon addition of water to the spreading areas.

Based on the observations that the water table rose regionally during the 1982 to 1985 time period, the constant head boundaries used during this study are not truly steady-state. However, it is actually the physical relief (i.e., the hydraulic gradient) of the water

table inside the model domain that is most important. As a result, a uniform regional rise in water levels does not affect the validity of the model produced during this study.

5. CONCLUSIONS

The best-case simulation scenario reproduces observed heads more accurately than previous simulations. The enhanced accuracy results from the addition of new deviation-corrected water level data and permeability information. The best model also represents a substantial improvement over a simulation that parameterized kriged permeability data. A small spatial correlation range and limited pump-test data are suggested as reasons for the inaccuracy of the geostatistically analyzed discretization of aquifer permeability.

The addition of water to the spreading areas may impart an eastward groundwater flow component in the vicinity of the SDA, based on simulated, best-case water levels. The modeled eastward flow component is supported by physical hydraulic head observations. However, observed water levels rose more dramatically during the 1982 to 1985 time period than the simulated heads. If the magnitude of the eastward flow component and hydraulic gradient in the RWMC area are considered important for contaminant transport calculations over the short time periods during and immediately after water is added to the spreading areas, then a more detailed analysis of spreading area infiltration rates, historic water levels, and flow model calibration is suggested.

6. REFERENCES

Ackermann, D.J., 1991. *Transmissivity of the Snake River Plain Aquifer at the Idaho National Engineering Laboratory, Idaho*, U.S.G.S. WRI-91-4059, 35 pp.

Magnuson, S.M., 1995. *Inverse Modeling for Field-Scale Hydrologic and Transport Parameters of Fractured Basalt*, INEL-95/0637, Lockheed Martin Idaho Technologies Co.

Magnuson, S.M. and A.J. Sondrup, 1998. *Development, Calibration, and Predictive Results of a Simulator for Subsurface Pathway Fate and Transport of Aqueous- and Gaseous-Phase Contaminants in the Subsurface Disposal Area at the Idaho National Engineering and Environmental Laboratory*. INEEL/EXT-97-00609, Lockheed Martin Idaho Technologies Co.

Vinsome, P.K.W. and G.M. Shook, 1993, *Multi-Purpose Simulation,* Journal of Petroleum Science and Engineering, Vol. 9, pp. 29-38.

Wood, T.W., 1989. *Preliminary Assessment of the Hydrogeology at the Radioactive Waste Management Complex, Idaho National Engineering Laboratory,* EGG-WM-8694, EG&G Idaho, Inc.

Wylie, A.H. and J.M. Hubbell, 1994, *Aquifer Testing of Wells M1S, M3S, M4D, M6S, M7S, and M10S at the Radioactive Waste Management Complex*, EDF ER-WAG7-26, Rev. 1, EG&G Idaho, Inc.

Wylie, A.H., 1996. *Pumping Test of Pit 9 Production Wells*, EDF INEL-96/171, Lockheed Martin Idaho Technologies Co.